

FLOW OF RAREFIED PLASMA AROUND A BODY

I. A. BOGASHCHENKO, A. V. GUREVICH, R. A. SALIMOV, and Yu. I. ÉIDEL'MAN

P. N. Lebedev Physics Institute, USSR Academy of Sciences; Nuclear Physics Institute, Siberian Division, USSR Academy of Sciences

Submitted June 10, 1970

Zh. Eksp. Teor. Fiz. 59, 1540–1555 (November, 1970)

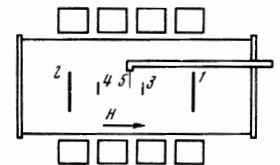
Langmuir probes were used to investigate in detail the structure of the perturbed zone in the vicinity of a disk placed in a stream of a rarefied plasma. The plasma stream was produced in a Q machine. The density, velocity, and temperature in the plasma stream as well as the surface potential and the position of the body in the stream were varied. The measurements and their comparison with theory have made it possible to establish the existence of ion acceleration in the self-consistent electric field produced in the plasma. At the same time, the longitudinal ion temperature is greatly decreased. The wake of the body has an oscillatory structure. An investigation of the damping of the oscillations has shown that collisions give rise to a gradual equalization of the longitudinal and transverse ion temperatures. It is shown that reversal of the sign of the potential of the body relative to the plasma has little effect on the structure of the perturbed zone behind the body. Reversal of the sign of the potential of another body situated in the perturbed zone of the first body greatly changes the structure of this zone in the region between the bodies. The measurement results agree with the theory.

1. INTRODUCTION

THE phenomena occurring when artificial satellites and rockets are placed in a stream of a rarefied plasma are of considerable interest^[1,2]. Experimental measurements in the ionosphere, magnetosphere and in cosmic space in the vicinity of the earth are quite complicated. There is therefore natural interest in an investigation of flow around bodies in laboratory conditions simulating the true flight conditions. The corresponding measurements performed by a number of authors^[3-9] have shown that the zone perturbed by the body has a number of important singularities, namely the occurrence of regions of rarefaction and condensation in the plasma^[3] (Hall, Kemp, Sellen), an oscillatory character of the perturbations at large distances behind the body^[5] (Barret), etc. No attempts were made, however, in these investigations to make a detailed quantitative comparison of the experimental results with theory. This is the purpose of the present investigation.

The complexity of such a problem lies, first of all, in the fact that it is necessary to have a stable and stationary stream of rarefied plasma flowing around the body. It is necessary, in addition, to have a sufficiently accurate idea of the properties of the plasma stream before it is perturbed by the body, namely the plasma density, the electron and ion temperatures, their translational velocities, and the character of the distribution functions. From this point of view, it is most advantageous to use an installation of the Q-machine type for study of streaming effects. In the latter, the plasma is produced by thermal ionization of potassium on a tungsten ionizer heated to $\sim 2000^\circ\text{K}$. The plasma is contained by a strong magnetic field and constitutes a cylindrical column bounded on one end by the ionizer and on the other by a cold electrode. In such a system, the plasma produced on the ionizer flows towards the cold electrode, on which it vanishes. The plasma parameters (its density, translational

FIG. 1. Diagram of setup: 1—ionizer, 2—anode, 3—disk 1, 4—disk 2, 5—probe.



velocities, and electron and ion temperatures) vary significantly, depending on the potentials and the temperature of the anode, and the intensity of vaporization. Within a wide range of variation of the parameters, the plasma stream is stable. It is relatively easy to perform various types of probe measurements in the installation. All this makes it possible to employ the Q machine quite effectively for an investigation of flow of rarefied plasma around a body¹⁾.

2. PROPERTIES OF PLASMA STREAM

The experiments were performed with the experimental setup described in detail by Buchel'nikova^[11]. Its diagram is shown in Fig. 1. The measurements were made with cylindrical probes 2 mm long and 0.25 mm in diameter. The probes could be moved along the axis of the installation and in a radial direction.

The properties of the plasma produced in the Q machine are determined to a considerable degree by the ion and electron currents from the ionizer. In our case, the experiments were performed in the regime when an electron layer was present, and the electron current from the ionizer was much larger than the ion current. In this case a layer of negative electric charge—an electron layer—is produced near the ionizer and reflects some of the electrons back to the ionizer. The thickness of this layer is of the order of the Debye radius D , i.e., it is much smaller than the dimensions

¹⁾The advantages ensuing from the use a Q machine for the investigation of flow of plasma around a body were recently pointed out in a paper by Korn et al. [10].

Table I.

$\dot{\rho}_{i_1}$, $\mu\text{A}/\text{cm}^2$	T , °K	H, Oe	n , cm^{-3}	ρ_{Hi} , cm	v_0/v_T	φ_0^*	$T_{e\perp}/T_{e\parallel}$, °K	l_0 , cm	l_1 , cm	Fig. No.
50	2150	1100	$1.5 \cdot 10^9$	0.35	2.0	3.2	160	0.6	40	3.4
30	2200	1100	$9 \cdot 10^8$	0.36	1.95	2.9	170	1.0	64	5a, 7
30	2200	1900	$7 \cdot 10^8$	0.21	2.6	6.0	100	0.8	110	5b
100	2200	1000	$6 \cdot 10^9$	0.39	1.0	0.4	500	0.7	6	6a. I
185	2155	1500	$8 \cdot 10^9$	0.26	1.2	0.7	390	0.4	4	6a. II
30	1970	1900	$9 \cdot 10^8$	0.20	1.9	2.7	160	0.8	46	6b. I
30	1880	1900	$3 \cdot 10^9$	0.19	0.8	0.15	520	1.3	7	6b. II

Note: $v_T = \sqrt{2TM^{-1}}$, $\varphi_0^* = -e\varphi_0/T$.

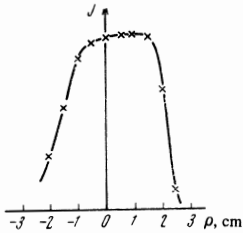


FIG. 2. Distribution of plasma along the radius of the column.

L of the setup ($D = 0.01$ cm, $L = 36$ cm). Behind the electron layer, the plasma is quasineutral, and the electron and ion densities n_e and n_i are close to each other, i.e., $n_e \approx n_i \approx n$. A typical radial distribution of the quasineutral plasma is shown in Fig. 2. The plasma density is maximal on the system axis and falls off towards the edges.

Under the influence of the electric field in the electron layer, the ions are accelerated and acquire a directional velocity v_0 . The distribution function of the ions is Maxwellian, but the longitudinal and transverse ion temperatures are, generally speaking, not equal. The transverse temperature $T_{i\perp}$ is close to the ionizer temperature T . The longitudinal ion temperature $T_{i\parallel}$ can be much smaller. The collisions between ions tend to equalize $T_{i\parallel}$ and $T_{i\perp}$, so that $T_{i\parallel}$ increases with increasing distance z from the ionizer: $T_{i\parallel} = T_{i\parallel}(z)$; at the same time, the temperature $T_{i\perp}$ decreases slightly. A detailed analysis of the question of the form of the distribution function of the ions and its deformation due to collisions is given in the Appendix.

The electron distribution function depends on the potential of the anode. Our measurements were carried out at negative anode potentials $\varphi_a \approx -7$ V, so that $-e(\varphi_a - \varphi_0)/T \gg 1$. In this case the electron distribution function is Maxwellian with a temperature T_e equal to the ionizer temperature T . This is well confirmed by probe measurements^[12].

The magnetic field H , which is directed along the symmetry axis, was varied from 1,000 to 2,000 Oe, the plasma density was $n \sim 7 \times 10^8 - 8 \times 10^9 \text{ cm}^{-3}$, the ionizer temperature T was varied from 1800 to 2200°K, the ion stream velocity v_0 ranged from 5×10^4 to 3×10^5 cm/sec (K^+ ions), and the plasma potential relative to the ionizer was $\varphi_0 \approx 0 - 1.5$ V. (These quantities are listed for the concrete experiments in Table I.)

The plasma was made to flow around a disk of radius $R_0 = 0.25$ cm. placed on the axis of the installation 10 cm away from the ionizer. In a number of experiments a second disk of 0.35 cm radius was placed 21 cm behind the first disk. The pressure of the neu-

Table II.

	Q machine	Ionosphere
R_0/D	$30 - 10 \gg 1$	$1000 - 50 \gg 1$
R_0/ρ_{He}	$200 - 300 \gg 1$	$100 - 200 \gg 1$
v_0/v_{Te}	$\sim 0.01 \ll 1$	$\sim 0.01 \ll 1$
v_0/v_T	$\approx 0.5 - 3$	$\approx 0.8 - 6$
R_0/ρ_{Hi}	$\approx 0.6 - 1.2$	$\approx 0.25 - 1.0$
R_0/l	$\approx 5 \cdot 10^{-2} - 10^{-3} \ll 1$	$\approx 5 \cdot 10^{-2} - 10^{-4} \ll 1$

tral gas in the apparatus was $p \sim 10^{-6}$ Torr. Therefore the mean free paths for the collisions with the neutrals were $l_n \sim 10^4$ cm; the neutrals could therefore be neglected. The mean free path for collision between charged particles was of the order of the setup dimensions, $l \sim 10 - 200$ cm. Collisions between the electrons could be neglected, since they did not change the Maxwellian distribution function of the electrons. The electron-ion collisions were also insignificant. To the contrary, collisions between ions greatly deform the ion distribution function, as was already noted above. Their role is considered in detail in the Appendix.

Let us now estimate the values of the parameters characterizing flow around the disk: the Debye radius is $D \sim (1 - 2) \times 10^{-2}$ cm, the ion Larmor radius $\rho_{Hi} = \sqrt{2T/M}/\omega_{Hi} \sim 0.4$ cm at $H = 1000$ Oe and $\rho_{Hi} \sim 0.2$ cm at $H = 2000$ Oe, the electron Larmor radius is $\rho_{He} \sim 10^3$ cm, the ion thermal velocity is $v_T = \sqrt{2TM^{-1}} \sim 1 \times 10^5$ cm/sec, and the electron thermal velocity is $v_{Te} = \sqrt{2T_e m^{-1}} \sim 3 \times 10^7$ cm/sec.

Table II lists the values of the dimensionless parameters characterizing flow around a body in a Q machine and in the ionosphere at altitudes $h \sim 200 - 1000$ km for bodies with dimensions $R_0 \approx 2$ m. It is seen from the presented data that the conditions of our experiments in the Q machine closely simulate real conditions in the ionosphere.

3. DISCUSSION OF RESULTS

Near Zone

The magnetic field greatly influences flow of plasma around a body at distances z larger than $\pi\rho_{Hi}v_0/v_T$, i.e., in our case at distances larger than 1-2 cm away from the disk. We consider here first the near zone $z \lesssim 1$ cm, where the influence of the magnetic field is negligible. Typical results of the measurement of the ion current to the probe in the near zone are shown in Figs. 3 and 4. Here $v_0 = 2.0 \times 10^5$ cm/sec, $T = 2150^\circ\text{K}$, $v_T = 1.0 \times 10^5$ cm/sec ($v_0/v_T = 2.0$), and $H = 1100$ Oe. The probe potential relative to the plasma is ≈ -2 V. The experimental points in Fig. 3 give the ratio

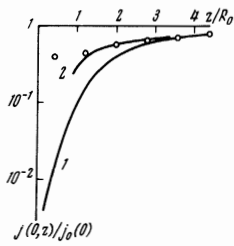


FIG. 3. Distribution of the plasma on the axis in the near zone behind the body. Points—experiment ($H = 1100$ Oe, $T = 2150^\circ\text{K}$, $J_{0i} = 50 \mu\text{A}/\text{cm}^2$, $v_0/v_T = 2.0$). Theoretical curves of $n(0, z)/n_0$: 1—“neutral approximation”; 2—with allowance for the influence of the electric field.

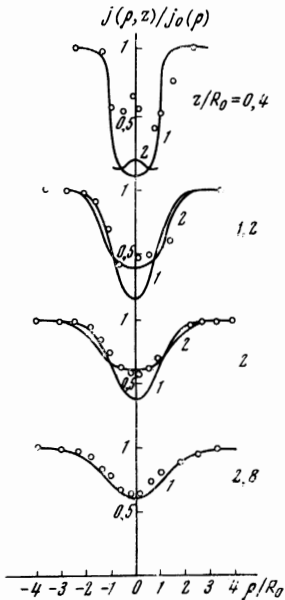


FIG. 4. Radial distribution of plasma in the near zone behind the body. Points—experiment ($H = 1100$ Oe, $T = 2150^\circ\text{K}$, $j_{0i} = 50 \mu\text{A}/\text{cm}^2$, $v_0/v_T = 2.0$). Theoretical plots of $n(\rho, z)/n_0$: 1—“neutral approximation”; 2—with allowance for the influence of the electric field.

$j(0, z)$, $j_0(0)$, where $j(0, z)$ is the current of ions to a probe located on the axis behind the body and $j_0(0)$ is the same ion current on the axis in front of the body. The abscissas represent the ratio z/R_0 , where R_0 is the radius of the disk. The points in Fig. 4 give the radial distribution $j(\rho, z)/j_0(\rho)$ at the fixed values of z/R_0 indicated on the figure.

Let us compare the calculation results with experiment. An approximate expression for the plasma distribution in the perturbed zone behind the disk was obtained in^[13] and in^[1], Sec. 5. In its derivation no account was taken of the influence exerted on the ion motion by the electric field produced in the perturbed plasma zone (the “neutral approximation”). Calculations with allowance for the influence of the field were performed in^[14-16]. It was shown that far from the body—at distances $z \gtrsim R_0 v_0/v_T$, the influence of the field, while noticeable, is not decisive. To the contrary, in the region close to the body, $z \ll R_0 v_0/v_T$, the influence of the electric field is very large; it leads to an appreciable increase of the plasma density. Analytic expressions for the plasma distribution in the region close to the disk, with allowance for the influence of the electric field on the motion of the ions, were obtained in^[2].

The calculated ratio $n(\rho, z)/n_0$ is represented by the solid curves in Figs. 3 and 4. Here $n(\rho, z)$ is the ion concentration in the unperturbed zone, n_0 is the concentration in the unperturbed plasma. Curves 1 of Figs. 3 and 4 are constructed in accordance with formulas (9) of^[13] or (2.24) of^[1], Sec. 5 (the “neutral

approximation”). Curves 2 were constructed in accordance with formulas (69) and (73) of^[2], which take into account the influence of the electric field.

We see that theory and experiment are in sufficiently good agreement. Far from the body, at $z \gtrsim R_0 v_0/v_T$, the “neutral approximation” is quite accurate. To the contrary, near the body, $z < R_0 v_0/v_T$, the role of the electric field is significant. The considerable discrepancy between the calculation and the experimental results can be observed only when the probe is closest to the body—at a distance of 1 mm from the surface of the disk. Here the current j/j_0 turns out to be larger by one order of magnitude than the calculated value n/n_0 . This is to be expected. The point is that the Debye radius increases noticeably in the region of strong rarefaction behind the body. This increases the effective surface of the probe that gathers the ions, leading to an increase of the ion current to the probe. In addition, at such short distances from the disk, the finite dimensions of the probe itself undoubtedly come into play, since its length (2 mm) is larger than the distance from the probe to the disk (1 mm). Allowance for the finite dimensions of the probe also leads to an increase in the ion current.

Let us note an important qualitative effect connected with the influence of the electric field on the ion motion, namely the increase of the concentration (or current) of the ions near the axis $\rho = 0$; this increase is seen both on the theoretical curve and on the experimental points of the upper figure in 4. This increase is a consequence of the focusing of the ions near the axis under the influence of the axially-symmetrical electric field attracting the ions.

Far Zone

Results of measurements of the ion current to the probe at large distances behind the disk are shown in Figs. 5–7. The experimental points on the figures give, as before, the ratio $j(\rho, z)/j_0(\rho)$, where $j_0(\rho)$ is the current of the ions to the probe in the unperturbed plasma. Figures 5 and 6 show the distribution of the ion current on the axis $\rho = 0$ behind the body. We see that at relatively large values of the ionizer temperature T and at small values of the current density j_{0i} from the ionizer, the plasma distribution has a clearly pronounced oscillatory character (Fig. 5). Such plasma oscillations in the perturbed zone behind the body were theoretically predicted in^[13] and in^[1] (Chap. III) and were observed experimentally by Barret^[5]. Figure 7 shows the distribution of the plasma along the radius ρ ; it also pulsates as a function of z/R_0 . Figures 5 and 6 clearly show the damping of the oscillations. With decreasing ionizer temperature T and with increasing ion current j_{0i} , the damping increases, and at $T \lesssim 1800^\circ\text{K}$ the distribution of the plasma behind the body acquires an almost monotonic character (Fig. 6). At large distances $z/R_0 \gtrsim 20-50$, the perturbation of the plasma is almost homogeneous with respect to z , i.e., a cylindrical wake is established, as it were, with a definite radial distribution of the plasma-perturbation.

These phenomena are physically quite understandable. Indeed, some of the ions become absorbed by the

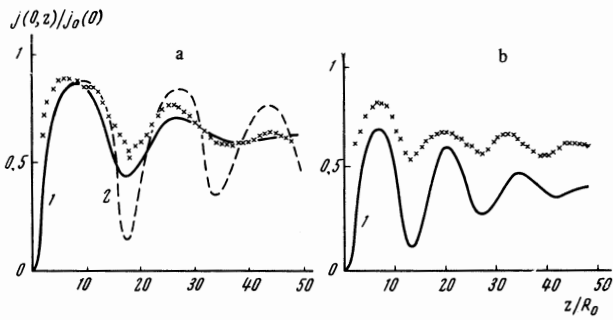


FIG. 5. Distribution of plasma along the axis in the far zone behind the body. Points—experiment; a— $H = 1100$ Oe, $T = 2200^\circ\text{K}$, $j_{0i} = 30 \mu\text{A}/\text{cm}^2$, $v_0/v_T = 1.95$; b— $H = 1900$ Oe, $T = 2200^\circ\text{K}$, $j_{0i} = 30 \mu\text{A}/\text{cm}^2$, $v_0/v_T = 2.6$. Theoretical $n(0, z)/n_0$ curves: 1—“neutral approximation” (formula (3)); 2—without allowance for the change of $T_{||}$ due to the collisions.

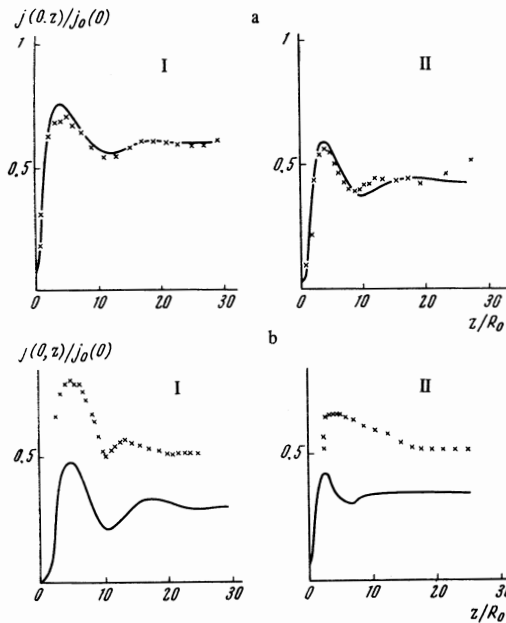


FIG. 6. Plasma distribution along the axis in the far zone behind the body. Points—experiment. a) I— $H = 1000$ Oe, $T = 2200^\circ\text{K}$, $j_{0i} = 100 \mu\text{A}/\text{cm}^2$, $v_0/v_T = 1.0$; II— $H = 1500$ Oe, $T = 2155^\circ\text{K}$, $j_{0i} = 185 \mu\text{A}/\text{cm}^2$, $v_0/v_T = 1.2$; b) I— $H = 1900$ Oe, $T = 1970^\circ\text{K}$, $j_{0i} = 30 \mu\text{A}/\text{cm}^2$, $v_0/v_T = 1.9$; II— $H = 1900$ Oe, $T = 1880^\circ\text{K}$, $j_{0i} = 30 \mu\text{A}/\text{cm}^2$, $v_0/v_T = 0.8$. The theoretical $n(0, z)/n_0$ curves were constructed in the “neutral approximation” (formula (3)).

body so that in the immediate rear of the body the ion concentration is minimal. With increasing distance from the body, the perturbation becomes smoothed out as a result of the thermal motion of the ions, and the concentration in the wake increases. However, the ions are not free, and they execute in the magnetic field a periodic motion with cyclotron frequency $\nu_{Hi} = \omega_{Hi}/2\pi = eH/2\pi Mc$. Therefore after a time $t_{Hi} = \nu_{Hi}^{-1}$ or else at a distance $\tau = \nu_{Hi} t_{Hi}$ behind the body, where

$$\tau = 2\pi v_0 / \omega_{Hi} = 2\pi M c v_0 / eH, \quad (1)$$

the picture should repeat, i.e., one should observe a decrease of the ion concentration. Here v_0 is the average ion velocity along the magnetic field. If $v_0 \gg v_{T||}$ ($v_{T||} = \sqrt{2T_{||}M}$ is the thermal velocity of the

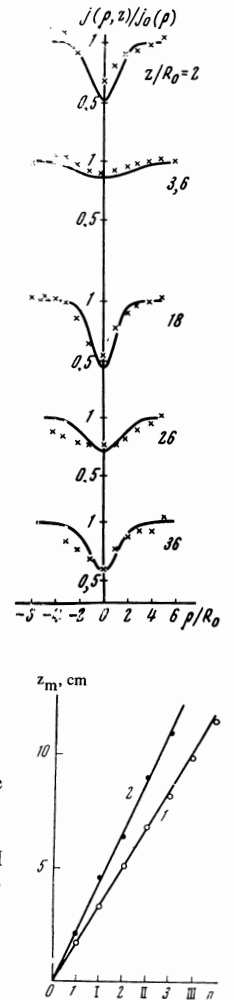


FIG. 7. Radial distribution of the plasma in the far zone behind the body. Points—experiment ($H = 1100$ Oe, $T = 2200^\circ\text{K}$, $j_{0i} = 30 \mu\text{A}/\text{cm}^2$, $v_0/v_T = 1.95$); the theoretical $n(\rho, z)/n_0$ curves were constructed in the “neutral approximation” (formula (2)).

FIG. 8. Distribution of the maxima (1, 2, 3, ...) and of the minima (I, II, III, ...) of the plasma density on the axis behind the body as a function of the magnetic field: 1— $H = 1900$ Oe, $T = 2200^\circ\text{K}$, $j_{0i} = 30 \mu\text{A}/\text{cm}^2$, $v_0/v_T = 2.6$; 2— $H = 1100$ Oe, $T = 2200^\circ\text{K}$, $j_{0i} = 30 \mu\text{A}/\text{cm}^2$, $v_0/v_T = 1.95$, z_m —distance from the ionizer.

ions along H), then practically all the ions move with velocities v_0 and the wake should oscillate with a period (1)^[1]. Such oscillations are seen in Fig. 5. Figure 8 shows the corresponding distribution of the maxima and minima of the current to the probe on the axis behind the disk. We see that the picture is indeed close to periodic. Measurement of the period of the oscillations (1) can serve as a good method of measuring the directional velocity of the ions^[12].

The thermal scatter with respect to the longitudinal velocities $v_{T||}$ leads to a damping of the oscillations. The damping increases with increasing longitudinal temperature $T_{||}$, i.e., with decreasing ratio $v_0/v_{T||}$. When $v_0/v_{T||} \lesssim 1$, the oscillations actually vanish. After the damping of the oscillations, a cylindrical wake is formed and spreads out only as a result of diffusion processes.

Let us now compare the results of a theoretical calculation with experiment. In the “neutral approximation,” i.e., neglecting the influence of the electric field on the ion motion, the concentration of the ions behind the disk is determined by the expression

$$\frac{n(\rho, z)}{n_0} = 2 \frac{\beta \bar{\gamma} \alpha}{\gamma \pi} \int_0^\infty dv' \exp \left\{ -a(v' - v_0)^2 - \frac{\beta \rho^2}{\xi^2} \right\} \times \int_{\nu_0 t}^\infty u' e^{-\beta u'} I_0 \left(\frac{2\beta \rho u'}{\xi} \right) du' + \frac{1}{2} [1 - \Phi(\sqrt{\beta} v_0)];$$

$$\begin{aligned}
 v' &= v_{\parallel} / v_T, & v_0' &= v_0 / v_T, \\
 u' &= v_{\perp} / v_T, & \rho_{Hi} &= v_T / \omega_{Hi}, & v_T &= \sqrt{2TM^{-1}}, & \alpha &= T / T_{\parallel}, & \beta &= T / T_{\perp}; \\
 I_0(t) &= \frac{1}{\pi} \int_0^{\pi} e^{-t \cos x} dx, & \Phi(t) &= \frac{2}{\sqrt{\pi}} \int_0^t e^{-x^2} dx, \\
 \xi &= 2\rho_{Hi} |\sin(z\sqrt{\beta} / 2\rho_{Hi} v')|.
 \end{aligned} \quad (2)$$

The derivation of formula (2) is perfectly analogous to the derivation given in^[1], Sec. 10. All that is taken into account additionally is that the ion distribution function is Maxwellian with different longitudinal and transverse ion temperatures T_{\parallel} and T_{\perp} (see Sec. 2). On the axis behind the disk ($\rho = 0$) formula (2) becomes much simpler and takes the form

$$\frac{n(0, z)}{n_0} = \sqrt{\frac{\alpha}{\pi}} \int_0^{\infty} \exp \left\{ -\alpha(v' - v_0')^2 - \frac{\beta R_0^2}{\xi^2} \right\} dv' + \frac{1 - \Phi(\sqrt{\alpha} v_0')}{2}. \quad (3)$$

The results of a numerical calculation of $n(0, z)/N_0$ by means of formula (3) are shown by the solid curves in Figs. 5 and 6. The longitudinal and transverse ion temperatures were determined here by the expressions given in the Appendix (see (A.9)). In particular, in the cases shown in Figs. 5 and 7, the longitudinal temperature T_{\parallel} is always much smaller than the transverse one; therefore in these cases, according to (A.10),

$$T_{\parallel} = T_{0\parallel} + \frac{z + z_1}{l_1} T, \quad T_{\perp} = T \left(1 - \frac{z + z_1}{2l_1} \right), \quad (4)$$

where z_1 is the distance from the ionizer to the disk. The temperature $T_{0\parallel}$ and the length l_1 , determined by formulas (A.2) and (A.10), are listed in Table I. In the cases represented in Fig. 6 (with the exception of 6b, I), the length l_1 is smaller than z_1 and therefore $T_{\parallel} = T_{\perp} = \frac{1}{3} T_{0\parallel} + \frac{2}{3} T$. In the case 6b, I we have $l_1 \sim z + z_1$, and the general formulas (A.9) were used to calculate T_{\parallel} and T_{\perp} . It is seen from the figures that the results of the calculations and the experiments are in sufficiently good agreement. There is good agreement in the general character of the curves, in the period of the oscillations, and in the damping of the oscillations. Of importance for the damping of the oscillations is the deformation of the distribution function and the change of the longitudinal temperature of the ions as a result of collisions, as indicated in the Appendix. For comparison, the dashed curve in Fig. 5a shows the distribution of the ion concentration in the wake in the absence of collisions, when the distribution function is given by (A.1). We see that during the period of the oscillations, which is determined by the average directional velocity of the ions (1), the collisions have no effect; on the other hand, the damping of the oscillations is determined by the longitudinal ion temperature T_{\parallel} , which depends appreciably on the collisions.

Notice should be taken of a certain quantitative discrepancy between the here-considered "neutral approximation" of the theory and the experiment. On the axis behind the disk, the experimental values of $j(0, z)/j_0(0)$ are higher than the calculated values of $n(0, z)/n_0$. The discrepancy increases with increasing magnetic field, or more accurately with increasing ratio of the body dimension R to the Larmor radius ρ_{Hi} of the ions. This is also seen in Fig. 9, which shows the dependence of the concentration perturbations on the axis $\rho = 0$ at large distances behind the

FIG. 9. Distribution of plasma on the axis behind the body as a function of the magnetic field; points—experiment. The theoretical $n(0, z)/n_0$ curve was constructed in the "neutral approximation" (formula (5)).

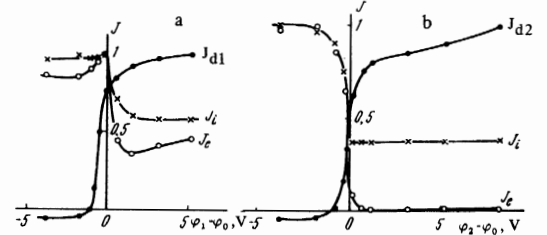
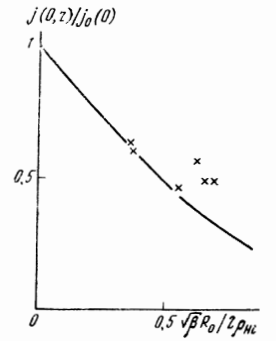


FIG. 10. Current to the disk (J_d) and ion and electron currents (J_i and J_e) to a probe located on the axis behind disk 1: a—as a function of the potential of disk 1, b—as a function of the potential of disk 2.

body (where the oscillations have already been damped out) on the magnetic field, or more accurately on the ratio $\sqrt{\beta}R_0/2\rho_{Hi}$. The point is that it follows from (3) that at large distances $z > \sqrt{\alpha}TV_0'$ (at $\sqrt{\alpha}V_0' > 1$) we have

$$n(0, z) / n_0 \approx 1 - \Phi(\sqrt{\beta}R_0 / 2\rho_{Hi}). \quad (5)$$

This quantity is represented by the solid curve in Fig. 9. The points stand for the experimentally measured ratio $j(0, z)/j_0(0)$. We see that the discrepancy between the experimental values and the theoretical curve (5) increases with increasing ratio $\sqrt{\beta}R_0/2\rho_{Hi}$. It can be assumed that the noted discrepancy is a consequence of the increase of the ion concentration on the axis $\rho = 0$ under the influence of the electric field, which was not taken into account in the derivation of formulas (2)–(5). This influence of the electric field on the motion of the ions was taken into account in the perturbation-theory approximation by Pitaevskii (see^[16] and^[1] Sec. 5). It was shown in^[17,18] that the field actually causes the concentration of the ions on the axis behind a body moving in a magnetic field to increase. With increasing ratio R_0/ρ_{Hi} , the plasma rarefaction in the wake of the body increases and the field assumes a larger role.

Change of Disk Potential. Captured Electrons

All the measurements described above were performed with the disk 1 at a sufficiently high negative potential relative to the plasma (see Fig. 1), usually with $\phi_1 - \phi_0 \approx -2$ V. As a result, the electrons had everywhere an equilibrium Maxwell-Boltzmann distribution. A change of the potential ϕ_1 of the disk 1 in the plasma stream led only to insignificant changes in the structure of the perturbed zone, namely, a change of $\phi_1 - \phi_0$ from -5 to -1 V changed the ion current to the probe in the perturbed zone by less than 10% (see Fig.

10). The reason for this was that the disk radius R_0 was much smaller than the Debye radius D in the unperturbed plasma. In this case the field of the disk is screened in the plasma and if the disk potential satisfies the condition $T \ll -e(\varphi_1 - \varphi_0) \ll T(R_0/D)^{4/3}$, then its changes should have only a slight effect on the plasma perturbation^[1,2].

The picture changes radically if the disk potential relative to the plasma reverses sign. In this case the electrons are freely absorbed by the body and their distribution is essentially no longer in equilibrium. This becomes particularly strongly manifest in the region of capture in the shadow of the disk 1, into which the electrons cannot fall without collisions.

The results of measurements of the ion and electron currents to a probe located on the axis in the shadow of the disk 1 (at a distance 1 cm from the surface) as functions of the potentials of disks 1 and 2 are shown in Fig. 10. It is seen from the figures that reversal of the sign of the potential $\varphi_1 - \varphi_0$ of the body relative to the plasma strongly influences the plasma concentration in the perturbed zone. The electron concentration is particularly strongly altered if disk 2 is at positive potential: the current to the probe then decreases by two orders of magnitude, whereas in the case of positive potential on disk 1 it decreases only by a factor of 2. The reason lies in the following.

A theoretical analysis shows that a negatively-charged region should be produced in the shadow zone of disk 1, and that the minimum of the potential is reached near the rear surface of the disk (see^[13] and^[1], Sec. 14). By virtue of this, reversal of the sign of the potential of disk 1 should not have a very strong effect on the concentration of the captured particles, since most of them cannot overcome the potential barrier and become absorbed on reaching the surface of the body. There is no negatively charged zone ahead of disk 2. Therefore, when the sign of the potential of disk 2 is reversed, the disk absorbs electrons freely, and the region between disks becomes almost completely free of electrons. This is clearly seen in Fig. 11. It follows also that reversal of the sign of the potential on the rear surface of a body moving in a magnetic field has relatively little effect on the structure of the perturbed zone. On the other hand, reversal of the potential of a body situated in the wake of another body leads to a strong change of the structure of the perturbed zone, resulting in a new perturbed region (with few electrons) stretched along the magnetic-field force lines that intersect both bodies.

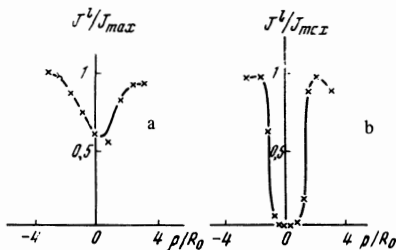


FIG. 11. Radial distribution of the electron current to the probe in the region $z = 1$ cm behind the disk 1: a—at positive potential of disk 1; b—at positive potential of disk 2.

Change of Disk Position

We have considered throughout the case in which the plane of the disk is perpendicular to the incoming plasma stream. Measurements were also performed with variation of the angle θ between the normal to the surface of the disk and the direction of the incoming stream. Figure 12 shows the results of measurements of the ion current J_i to the disk as a function of the angle θ ($j_{oi} = 33 \mu A/cm^2$, $T = 2150^\circ K$, $H = 1100$ Oe, $v_0/v_T = 1.9$). The dashed curve represents the ratio $J_N(\theta)/J_0$ calculated for the experimental conditions in the ‘neutral approximation’ (see^[1], formula (10.8)); solid curve 1 shows the same with allowance for the influence of the electric field on the motion of the ions in the quasineutral region of the plasma ($J_i(\theta)/J_0$, see^[2], formula (47)); curve 2 takes into account the finite thickness of the double layer at the disk surface ($J_0(\theta) = J_i(\theta) + \delta J$; the increment δJ is given by formula (97) of^[2], the potential of the disk relative to the plasma was $\varphi = \varphi_1 - \varphi_0 = -2.6$ V; plasma density $n \approx 10^9$ cm⁻³, i.e., $-e\varphi/T = 13$, $z_0/D = \sqrt{\pi}R_0/D = 40$). We see that at $\theta \approx 90^\circ$ the electric field has a strong influence on the ion current.

The current of electrons to the disk (at $\varphi > 0$) is proportional to $\cos \theta$ up to values of θ close to 90° . This is perfectly understandable, for the Larmor radius of the electrons is very small ($\rho_{He} \approx 2 \times 10^{-3}$ cm), so that the current is determined only by the cross-sectional area of the body in the plane perpendicular to the magnetic field.

APPENDIX

INFLUENCE OF COLLISIONS ON THE ION DISTRIBUTION FUNCTION

The distribution function of the ions in a quasineutral plasma of a Q machine in the absence of collisions is given by^[12]

$$f = \frac{M}{2\pi T} \exp\left\{-\frac{Mv_{\perp}^2}{2T}\right\} F(v_{\parallel}),$$

$$F(v_{\parallel}) = \begin{cases} \frac{j_{oi}M}{T} \exp\left(-\frac{Mv_{\parallel}^2}{2T} - \frac{e\varphi_0}{T}\right), & v_{\parallel} \geq \sqrt{-2e\varphi_0/M}, \\ 0, & v_{\parallel} < \sqrt{-2e\varphi_0/M}. \end{cases} \quad (A.1)$$

Here M is the mass of the ions, v_{\parallel} their velocity along the system axis, v_{\perp} the velocity in a plane perpendicular to the axis, φ_0 the potential difference between the

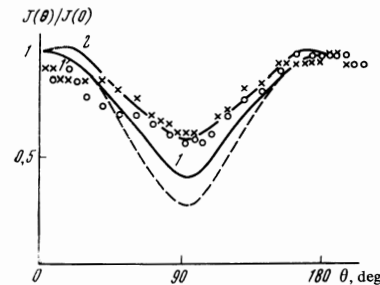


FIG. 12. Ion current to the disk as a function of the angle θ between the normal to the plane of the disk and the direction of the incoming stream. X, O—streams on opposite sides of the disk—the disk was rotated through 360° .

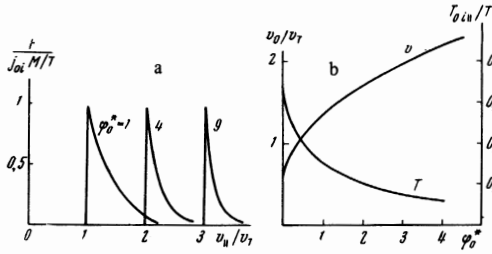


FIG. 13. a—Ion distribution function with respect to the longitudinal velocities in a quasineutral plasma; b—dependence of the average translational velocity v_0/v_T and of the longitudinal temperature $T_{0i||}/T$ of the ions on the quasineutral-plasma potential.

quasineutral plasma and the ionizer (in the here-considered case of an electron layer, $\varphi_0 < 0$). The distribution functions $F(v_{||})$ are shown in Fig. 13a.

The average translational velocity of the ions is

$$v_0 = \frac{\sqrt{2T/\pi M} e^{-\varphi_0^*}}{1 - \Phi(\sqrt{\varphi_0^*})}, \quad \varphi_0^* = -\frac{e\varphi_0}{T}, \quad \Phi(t) = \frac{2}{\sqrt{\pi}} \int_0^t e^{-x^2} dx.$$

At $\varphi_0^* \gg 1$, the translational velocity of the ions $v_0 \approx \sqrt{-2e\varphi_0/M}$ is much larger than their thermal velocity. The transverse ion temperature, as seen from (A.1), equals the ionizer temperature. The distribution function (A.1) is not Maxwellian in the direction along the system axis. In this case one can speak only of the effective longitudinal ion temperature $T_{0i||} = M(\overline{v_{||}^2} - v_0^2)$, given by

$$\frac{T_{0i||}}{T} = 1 + \frac{2\sqrt{\varphi_0^*} e^{-\varphi_0^*}}{\sqrt{\pi}[1 - \Phi(\sqrt{\varphi_0^*})]} - \frac{2}{\pi} \frac{e^{-2\varphi_0^*}}{[1 - \Phi(\sqrt{\varphi_0^*})]^2}. \quad (\text{A.2})$$

The temperature $T_{0i||}$ is smaller than T . It decreases with increasing φ_0^* , i.e., with increasing translational velocity v_0 , with $T_{0i||} \approx T^2/Mv_0^2$ when $\varphi_0^* \gg 1$. The dependence of the translational velocity v_0 and of the effective ion temperature $T_{0i||}$ on the potential φ_0^* of the quasineutral plasma is shown in Fig. 13b²⁾. The values of $T_{0i||}$, v_0 , and φ_0^* for the concrete conditions under which the experiments were performed are listed in Table I.

The distortion of the ion distribution function as a result of the collisions is described by the kinetic equation

$$v \cos \theta \frac{\partial f}{\partial z} = S(f). \quad (\text{A.3})$$

Here S is the integral of ion-ion and ion-electron collisions, $f = f(z, v, \theta)$, where z is the distance from the ionizer, v is the modulus of the velocity, and θ is the angle to the instrument axis.

Let us consider first a region of z sufficiently close to the ionizer, when the length l_0 , which characterizes the influence of the collisions, is larger than z : $l_0 > z$. In this region of z , appreciable changes of the initial distribution function (A.1) can occur only at velocities $v \cos \theta \sim v_0$, where the gradient of the initial distribution function is very large: $\partial f / \partial v_{||} \rightarrow \infty$ (see Fig. 13a). Then the collisions with the electrons are immaterial, and in addition the principal role is assumed by the change of the angular part of the distribution function.

²⁾The potential φ_0^* is determined by the temperature of the ionizer and by the electron and ion currents [12].

Therefore, in a coordinate system moving with velocity $v_0 \approx \sqrt{-2e\varphi_0/M}$ along the z axis, using the Landau collision integral for the ion-ion collisions, we can write S in the form

$$S = \frac{\alpha}{\sin \theta} \frac{\partial}{\partial \theta} \left(\sin \theta \frac{\partial f}{\partial \theta} \right). \quad (\text{A.4a})$$

At small values $v < v_T$, which play the major role, we have

$$\alpha = \frac{v_i(v)}{2} H\left(\frac{v}{v_T}\right) = \frac{8\pi e^4 j_{oi} \ln \Lambda}{3MTv^2} = \frac{\alpha_0}{v^2}, \quad (\text{A.4b})$$

$$\alpha_0 = \frac{8\pi e^4 j_{oi} \ln \Lambda}{3MT}.$$

Here $\ln \Lambda$ is the Coulomb logarithm. We took into account the fact that at small v the Landau collision integral has a linear character and is determined by the expressions given, for example, in [19, 20]. The ion concentration in the plasma is expressed in this case with the aid of formula (A.1) in terms of the ion current j_{oi} and the ionizer temperature T .

On the boundary $z = 0$, in the same coordinate system, the distribution function (A.1) is written in the form

$$f(0, v, \theta) = \frac{M^2 j_{oi}}{2\pi T^2} \varphi(\cos \theta, 0) \exp\left(-\frac{Mv^2}{2T} - \frac{Mvv_0}{T} \cos \theta\right),$$

$$\varphi(x, 0) = \begin{cases} 1, & x > 0, \\ 0, & x \leq 0. \end{cases} \quad (\text{A.5})$$

With allowance for the expressions (A.4), Eq. (A.3) takes the form

$$v_0 \frac{\partial f}{\partial z} = \frac{\alpha_0}{v^2} \frac{\partial}{\partial x} \left[(1 - x^2) \frac{\partial f}{\partial x} \right], \quad x = \cos \theta.$$

This equation contains v only as a parameter. Its solution under the boundary conditions (A.5) is given by

$$f(z, v, \theta) = \frac{M^2 j_{oi}}{4\pi^{3/2} T^2 \sqrt{t}} \exp\left\{-\frac{Mv^2}{2T}\right\} \int_0^\infty \exp\left\{-\frac{(x-x_0)^2}{4t} - x_0 \frac{Mvv_0}{T}\right\} dx_0,$$

$$t = z \frac{\alpha_0}{v_0 v^2}, \quad x = \cos \theta. \quad (\text{A.6})$$

We have taken into account here the fact that only small values of x are of practical interest ($x^2 \ll 1$).

The distribution function with respect to the velocity $v_{||} = v \cos \theta$ is determined by integrating f with respect to the transverse velocity

$$F(z, v_{||}) = 2\pi \int f(z, v, \theta) |_{\cos \theta = v_{||}/v} v dv. \quad (\text{A.7})$$

Taking into account the concrete form (A.6) of the function f , we can show that the distribution function (A.7) is sufficiently well approximated by the simple expression

$$F(z, v_{||}) = \frac{M j_{oi}}{2T} \left[1 + \Phi\left(\frac{u}{\beta}\right) \right] \begin{cases} e^{-u}, & u \geq 0 \\ 1, & u < 0 \end{cases}. \quad (\text{A.8})$$

$$u = \frac{v_{||}}{T/Mv_0^2}, \quad \beta = \frac{2M\sqrt{\alpha_0 v_0 z}}{T} = \sqrt{\frac{z}{l_0}}, \quad l_0 = \frac{3T_s}{32\pi e^4 j_{oi} M v_0 \ln \Lambda}.$$

By definition, $z < l_0$, so that $\beta < 1$. As $\beta \rightarrow 0$, the distribution function (A.8) coincides with (A.1) if $v_{||} < v_0$ (we recall that the function (A.8) is written in a coordinate system moving with velocity $v_0 \approx \sqrt{-2e\varphi_0/M}$). However, the smearing of the distribution function in the vicinity of its sharp initial boundary

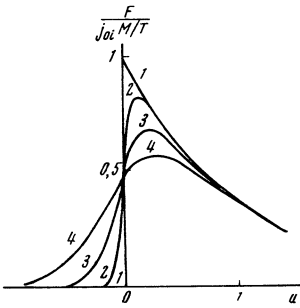


FIG. 14. Distribution function of the ions with respect to the velocity $u = v_{\parallel} / (T/Mv_0^2)$ for different z/l_0 : 1-0, 2-0.01, 3-0.1, 4-0.35.

turns out to be appreciable even at small values $\beta \sim 0.1$. This is seen from Fig. 14, which shows the function $F(u)$ for different values of the parameters β (A.8). At $\beta \sim 0.5-1$, the distribution function with respect to the velocity v_{\parallel} is already close to Maxwellian with a longitudinal temperature $T_{i\parallel} \approx T_{oi\parallel}$, where the temperature $T_{oi\parallel}$ is determined by the formula (A.2). The values of the length l_0 for the characteristic conditions of our experiments are indicated in Table I. We see that l_0 is always smaller than the distance from the ionizer to the disk, so that by the time the flow around the body begins the distribution function (A.1) always has time to turn into a Maxwellian function with $T_{i\parallel} \approx T_{i\perp}$.

The subsequent transformation of the ion distribution function as a result of collisions reduces simply to a gradual equalization of the longitudinal and transverse ion temperatures $T_{i\parallel}$ and $T_{i\perp}$. Using the results of Kogan^[21] (transforming in them from the time t to z/v_0), we find that the temperatures $T_{i\parallel}$ and $T_{i\perp}$ at any point z are given by the equations

$$\frac{dT_{i\parallel}}{dz} = \frac{4\sqrt{\pi}e^2 j_{oi} \ln \Lambda}{v_0^2 \sqrt{M}} \frac{\sqrt{T_{i\parallel}}}{T_{i\perp} - T_{i\parallel}} \left[-3 + \left(3 \sqrt{\frac{T_{i\parallel}}{T_{i\perp} - T_{i\parallel}}} + \sqrt{\frac{T_{i\perp} - T_{i\parallel}}{T_{i\parallel}}} \right) \arctg \sqrt{\frac{T_{i\perp} - T_{i\parallel}}{T_{i\parallel}}} \right], \quad T_{i\perp} = T - \frac{T_{i\parallel} - T_{oi\parallel}}{2}. \quad (\text{A.9})$$

If $T_{i\parallel} < 0$ (more accurately, $T_{i\parallel} < 0.5$ T), then the change of the transverse temperature can be neglected in first approximation, and the formulas in (A.9) take the simple form

$$T_{i\parallel} = T_{oi\parallel} + \frac{z}{l_1} T_s, \quad T_{i\perp} = T \left(1 - \frac{z}{2l_1} \right), \quad (\text{A.10})$$

$$l_1 = T^{3/2} \left(\frac{v_0}{v_r} \right)^2 / \pi^{3/2} \sqrt{M} e^2 j_{oi} \ln \Lambda, \quad v_r = \sqrt{\frac{2T}{M}}, \quad \frac{l_1}{l_0} = \frac{32\sqrt{2}}{3\sqrt{\pi}} \left(\frac{v_0}{v_r} \right)^3$$

l_1 is much larger than l_0 . Its characteristic values are also listed in Table I³⁾. If $z \gg l_1$, then, as is clear from (A.9), we have $T_{i\parallel} = T_{i\perp} = \frac{2}{3} T + \frac{1}{3} T_{oi\parallel}$.

³⁾In the numerical calculations we assumed $\ln \Lambda = 7$.

The authors are indebted to N. S. Buchel'nikova and L. P. Pitaevskii for a useful discussion, and L. V. Pariiskaya for the numerical calculations.

¹Ya. L. Al'pert, A. V. Gurevich, and L. P. Pitaevskii, *Iskusstvennye sputniki v razrezhennoi plazme (Artificial Satellites in a Rarefied Plasma)*, Nauka, 1964.

²A. V. Gurevich, L. P. Pitaevskii, and V. V. Smirnova, *Usp. Fiz. Nauk*, **99**, 3 (1969) [*Sov. Phys.-Usp.* **12**, 595 (1970)].

³P. F. Hall, R. F. Kemp, and J. M. Sellen, *AIAA Journ.*, **2**, 1032 (1964).

⁴E. D. Knechtell and W. G. Pitts, *AIAA Journ.*, **2**, 1148 (1964).

⁵P. J. Barret, *Phys. Rev. Lett.*, **13**, 742 (1964).

⁶F. J. F. Osborne, M. P. Bachynski, and M. A. Kasha, *URSI Spring Meeting, Washington, 1965*, Preprint 626.

⁷W. A. Clayden and C. V. Hurdle, *Rarefied Gas Dynamics*, G. L. Brundin ed., Academic Press, 1966, p. 1717.

⁸N. Kawashima and S. Mori, *Phys. Fluids*, **9**, 700, 1966; *AIAA Journ.*, **6**, 110 (1966).

⁹V. V. Skvortsov and L. V. Nosachev, *Kosmicheskie issledovaniya (Space Research)* **6**, 228, 855 (1968).

¹⁰P. Korn, T. C. Marshall, and S. P. Schlesinger, Preprint No. 47, Columbia Univers., N. Y., 1969.

¹¹N. S. Buchel'nikova, *Teplofizika vysokikh temperatur (High Temperature Physics)* **2**, 309 (1964).

¹²A. V. Gurevich, R. A. Salimov, and N. S. Buchel'nikova, *ibid.* **7**, 852 (1969).

¹³A. V. Gurevich, in: *Iskusstvennye sputniki Zemli (Artificial Earth Satellites)* **7**, 101 (1961).

¹⁴L. P. Pitaevskii and V. Z. Kresin, *Zh. Eksp. Teor. Fiz.* **40**, 271 (1961) [*Sov. Phys.-JETP* **13**, 185 (1961)].

¹⁵Yu. N. Panchenko and L. P. Pitaevskii, *Geomagnetism i aeronomiya* **4**, 256 (1964).

¹⁶N. I. Bud'ko, *ibid.* **6**, 1008 (1966).

¹⁷L. P. Pitaevskii, *ibid.* **1**, 194 (1961).

¹⁸V. V. Vas'kov, *Zh. Eksp. Teor. Fiz.* **50**, 1124 (1966) [*Sov. Phys.-JETP* **23**, 748 (1966)].

¹⁹A. V. Gurevich, *ibid.* **40**, 1825 (1961) [**13**, 1282 (1961)].

²⁰D. V. Sivukhin, in: *Voprosy teorii plazmy (Problems of Plasma Theory)*, No. 4, 1964, p. 81.

²¹V. I. Kogan, *Fizika plazmy i problemy upravlyayemykh termoyadernykh reaktzii (Plasma Physics and Problems of Controlled Thermonuclear Reactions)* **1**, 130 (1958).

Translated by J. G. Adashko